4390 J. Med. Chem. 2010, 53, 4390–4398
DOI: 10.1021/jm100445e

Journal of Medicinal Chemistry Article

Turning off Transcription of the *bcl-2* Gene by Stabilizing the *bcl-2* Promoter Quadruplex with Quindoline Derivatives

Xiao-Dong Wang,[†,‡] Tian-Miao Ou,[†,‡] Yu-Jing Lu,[‡] Zeng Li,[‡] Zheng Xu,[‡] Chen Xi,[‡] Jia-Heng Tan,[‡] Shi-Liang Huang,[‡] Lin-Kun An,[‡] Ding Li,[‡] Lian-Quan Gu,*[,‡] and Zhi-Shu Huang*[,‡]

[‡]*School of Pharmaceutical Sciences, Sun Yat-sen University, Guangzhou 510006, China.* [†]*These authors contributed equally to this paper.*

Received December 21, 2009

Human *bcl-2* gene is an apoptosis-related oncogene containing a GC-rich sequence which is located upstream from P1 promoter and has the potential to form G-quadruplex structures. However, the regulatory role of the quadruplex and the effect of its ligands on *bcl-2* have not been clarified. Here, we demonstrated that the G-quadruplex structure was disrupted when partial mutation of G → A was made, resulting in a 2-fold increase in basal transcriptional activity of *bcl-2* promoter. Quindoline derivatives, the highly active G-quadruplex ligands developed by our group, could significantly suppress *bcl-2* transcriptional activation but had less effect on mutated *bcl-2* transcription. These results provided direct evidence that G-quadruplex structure formed in *bcl-2* promoter region could function as a transcriptional repressor element, and G-quadruplex specific ligands could regulate the transcription of *bcl-2* through stabilization of quadruplex structure. The results further indicated that quindoline derivatives could induce apoptosis of HL-60 tumor cells.

Introduction

Quadruplexes, a family of DNA structures in the human genome, have been characterized in oncogenes, which may play for switching genes on or off in situ and become promising anticancer drug targets.[1] G-quadruplex, the stacking of tetrameric arrangement of guanines, formed transiently in genomic DNA, notably in gene promoters, could help regulation of gene transcription in living cells. The first direct evidence for G-quadruplex located in the P1 promoter of *c-myc* gene acting as a repressor of transcription was reported in 2002.[2] G-quadruplex in the promoter regions of *PDGF* and *KRAS* gene could also regulate the transcription through their binding to G-quadruplex ligands.[3,4] G-quadruplex in *c-kit* gene promoter has also been studied thoroughly, while a small molecule disrupting G-quadruplex is shown with the ability of enhancing *c-kit* expression.[5−7] Moreover, many other genes have been proved with the G-quadruplex forming potentials in their promoter regions, such as *bcl-2*, *VEGF*, *HIF-1*α, *Ret*, and *c-myb*.[8−15] P1 promoter of *bcl-2* gene is one of the two major promoters, which is located at 1386 to 1423 base pairs upstream of the translation start site (Figure 1).[16] A 39-base-pair GC-rich sequence (Pu39) upstream from the P1 promoter might play an important role in the regulation of *bcl-2* gene transcription.[17,18] This guanine-rich DNA strand has the potential to form multiple G-quadruplex structures in vitro, which could be stabilized by specific ligands and thus might cause down-regulation for the transcription of *bcl-2* gene.[11,12,19,20]

Human *bcl-2* gene, one member of the proto-oncogene *bcl-2* family, is overexpressed in various human cancers, including B-cell and T-cell lymphomas, nonsmall cell lung cancer, myeloma, and melanoma.[21−23] Its product Bcl-2 protein is a mitochondrial membrane protein, which exists in delicate balance with other related proteins and takes part in the controlling of programmed cell death. Its overexpression in the tumor cell not only functions as an apoptosis inhibitor[24] but also causes resistance to chemotherapy or radiotherapy-induced apoptosis.[25,26] Because of the apoptosis-related functions of Bcl-2 and the regulatory role of G-quadruplex on *bcl-2*, the G-quadruplex ligands may become potential antitumor agents.

The natural product cryptolepine and its quindoline derivatives have been verified to induce/stabilize the G-quadruplex structures in telomeric DNA[27−30] and *c-myc* NHE III_1 DNA and shown significant effects on the biological functions of these genes.[28,31] Especially, quindoline derivative **4** (SYUIQ-05), synthesized by our group, has been displayed with delayed-apoptosis inducing property in leukemia cells.[32] For the quindoline derivatives, an amino group in the side chain has been proved to be more effective than hydroxyl group for interacting with G-quadruplex.[29,31] Furthermore, the introduction of a positive charge by methylation at the 5-N position of 7-fluorinated quindoline derivatives could significantly improve their binding affinity to G-quadruplex and inhibitory effect on the telomere biological functions.[30] Besides, it is testified that 10*H*-indolo[3,2-*b*]quinoline analogues have G-quadruplex stabilizing and telomerase inhibiting abilities.[33,34] In the present study, the effects of quindoline derivatives from our group (Figure 2) were evaluated. Here, **1** (SYUIQ-01) is a quindoline derivative with a hydroxyl group in the side chain, which has been reported as a weak active G-quadruplex ligand.[31] **2** (SYUIQ-F05) is also a quindoline derivative with an amino group in its side chain and a fluorine at its 7-position and **3** (SYUIQ-FM05) is a cryptolepine

*To whom correspondence should be addressed. Phone: 8620-39943056 (Z.-S.H.); 8620-39943055 (L.-Q.G.). Fax: 8620-39943056 (Z.-S.H. and L.-Q.G.). E-mail, ceshzs@mail.sysu.edu.cn (Z.-S.H.); cesglq@mail.sysu.edu.cn (L.-Q.G.).

 Published on Web 05/18/2010

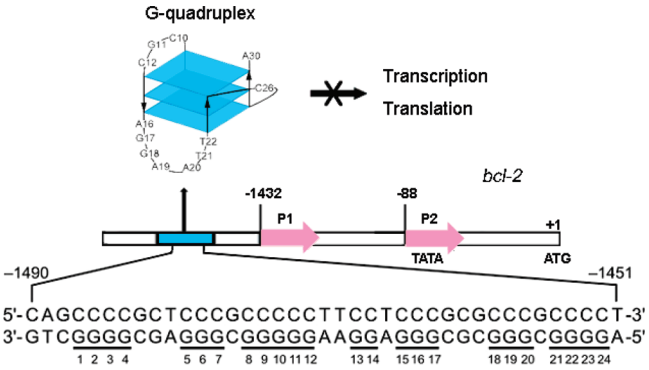

Figure 1. G-rich strand in the *bcl-2* promoter and proposed biological function for the G-quadruplex forming in this region.

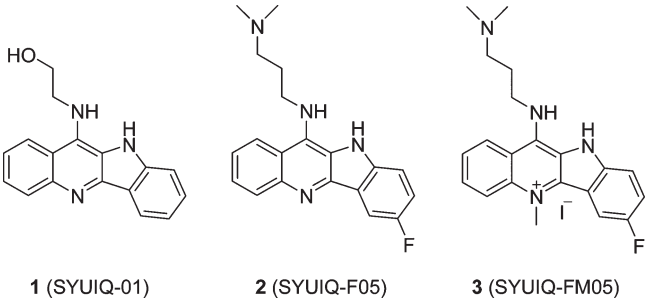

Figure 2. Structures of quindoline derivatives.

derivative (methylated quindoline derivative) with a same side chain as **2**, and both of them have shown great G-quadruplex binding activity.[30] These three derivatives were used to investigate their interaction with GC-rich sequence located upstream of *bcl-2* P1 promoter and their effects on *bcl-2* biological functions with various techniques, including polymerase chain reaction stop assay (PCR[a] stop assay), surface plasmon resonance (SPR), fluorescence resonance energy transfer-melting (FRET-melting), luciferase activity assay, real-time reverse transcription PCR (RT-PCR), Western blot, and flow cytometry analysis. The results indicated that the formation of G-quadruplex structure in *bcl-2* gene could turn off *bcl-2* transcription, and quindoline derivatives could stabilize the G-quadruplex structures in the upstream region of *bcl-2* P1 promoter, thus down-regulate P1 promoter activity and transcription/translation of *bcl-2* gene, leading to apoptosis of HL-60 cell. Moreover, the comparison of these three derivatives indicated that **3** had the most significant effect on down-regulation of *bcl-2* gene and induction of HL-60 cell apoptosis.

Results

Inhibition of Amplification in the Promoter Region of *bcl-2* by the Quindoline Derivatives. PCR stop assay was used in the quantitative screening of the quindoline derivatives for their interaction with *bcl-2*. Single-strand oligomer Pu39 was induced to form G-quadruplex structure in the presence of the ligands, and the G-quadruplex could block hybridization with its complementary strand overlapping the last G repeat. As a result, the 5′ to 3′ extension catalyzed by *Taq* polymerse was inhibited and the final double-stranded DNA PCR product could not be detected.[31,35]

The inhibitory activity of the derivatives on the hybridization of Pu39 or MutPu39 with its complementary strand was demonstrated by IC_{50} values, which were calculated using optical density read from LabWorks software and listed in Table 1. MutPu39 was used as a control with three G-tracts mutated, which totally eliminated the possibility of forming G-quadruplex. **1** and **2** showed IC_{50} values above 100 μM for MutPu39, which indicated that these two quindoline derivatives could not inhibit Pu39 hybridization with its complementary strand by interacting with *Taq* polymerase or duplex DNA. Although **3** still showed inhibitory activity on MutPu39, its IC_{50} value (19.7 μM) was much higher than that on Pu39 (1.11 μM), which indicated the effect of **3** on *bcl-2* G-quadruplex possessed a major role in this procedure. Moreover, the three quindoline derivatives had obvious different IC_{50} values for Pu39. **3** showed greatest inhibitory activity on Pu39 hybridization with an IC_{50} of 1.11 ± 0.12 μM, while **2** demonstrated a similar activity at the concentration of approximate 75 μM. In comparison, even at the concentration of 100 μM, the weakest derivatives **1** still could not obviously inhibit Pu39 hybridization. In particular, as shown in Figure 3, compound **3**, at the concentration of 1 μM, showed

Table 1. IC_{50} (μM) Values of Derivatives in the PCR Stop Assay

	3	2	1
Pu39	1.11 ± 0.12	74.4 ± 9.3	> 100
MutPu39	19.7 ± 3.0	> 100	> 100

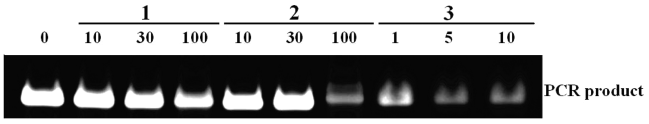

Figure 3. Effects of the derivatives on amplification of *bcl-2* promoter region using PCR stop assay. Three derivatives at increasing concentrations as indicate in the Figure (10, 30, and 100 μM for **1** and **2**, 1, 5, and 10 μM for **3**) were added into the PCR systems and the double-stranded PCR products (55 bp) were separated using 16% polyacrylamide gel.

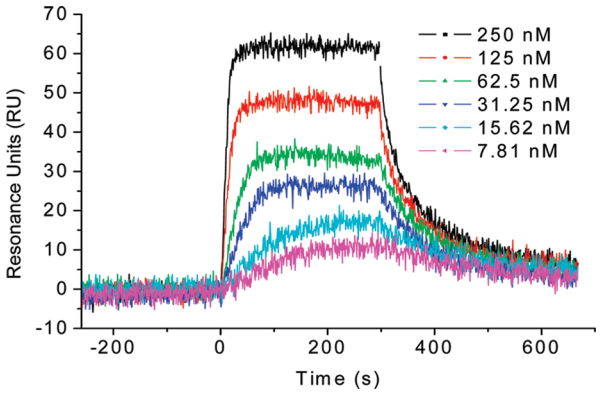

Figure 4. SPR sensorgrams for binding of **3** to the immobilized *bcl-2* G-quadruplex. In the plot, ligand concentrations in the flow solutions were 7.81, 15.62, 31.25, 62.5, 125, and 250 nM for the curves from the bottom to the top.

[a]Abbreviations: PCR, polymerase chain reaction; SPR, surface plasmon resonance; FRET, fluorescence resonance energy transfer; RT-PCR, reverse transcription PCR; PDGF, platelet-derived growth factor; VEGF, vascular endothelial growth factor; HIF-1α, hypoxia inducible factor-1α; NHE III_1, nuclease-hypersensitivity element III_1; IC_{50}, half maximal inhibitory concentration; k_a, association constant; k_d, dissociation constant; K_D, equilibrium dissociation constant; T_m, melting temperature; GAPDH, glyceraldehyde phosphate dehydrogenase; PARP, poly ADP-ribose polymerase; MTT, 3-(4,5-dimethylthiazol-2-yl)-2,5-diphenyltetrazolium bromide; SAR, structure−activity relationship; EtBr, ethidium bromide; FAM, 6-carboxyfluorescein; TAMRA, 6-carboxytetramethyl-rhodamine; DEPC, diethyl pyrocarbonate.

Table 2. Kinetic Parameters Determined with SPR Spectroscopy [a]

	3		2		1	
	bcl-2	duplex	*bcl-2*	duplex	*bcl-2*	duplex
k_a (M^{-1} s^{-1})	2.29×10^5	2.23×10^5	1.20×10^5	1.66×10^5	8.65×10^4	5.92×10^3
k_d (s^{-1})	7.28×10^{-3}	0.06	0.02	0.08	0.13	0.02
K_D (M)	3.18×10^{-8}	2.69×10^{-7}	1.67×10^{-7}	4.82×10^{-7}	1.50×10^{-6}	3.38×10^{-6}

[a] k_a is association constant, while k_d is dissociation constant. K_D denotes the equilibrium dissociation constant, given by k_d / k_a.

Table 3. T_m Values of the Oligomer MidG4 Incubated with Different Derivatives

	no derivative	3	2	1
T_m/°C	48.5 ± 0.7	76.9 ± 1.8	65.1 ± 0.8	51.5 ± 1.0

a significant inhibitory activity on Pu39 hybridization, while its analogue, compound **2**, could not inhibit the hybridization even at the concentration of 30 μM.

Binding Affinity of the Quindoline Derivatives to G-Quadruplex DNA. SPR is a useful technique to monitor molecular reactions in real time, which has been applied to investigate the interactions between small molecular ligands and human telomeric G-quadruplex.[36−41] Here, SPR experiments were carried out in order to quantitatively determine the kinetic constants of the derivatives binding to either G-quadruplex or duplex DNA. Figure 4 shows the SPR sensorgrams of **3** binding to the immobilized *bcl-2* G-quadruplex at the concentration of 7.81, 15.62, 31.25, 62.5, 125, and 250 nM. Then K_D was calculated by global fitting of the kinetic data from various concentrations of quindoline derivatives using 1:1 Langmuir binding (Table 2). As the data show, **3** had the highest binding affinity to *bcl-2* G-quadruplex with a K_D value of 32 nM, while the binding ability of **2** was medium (K_D value was about 167 nM) and **1** was the lowest (K_D value was about 1500 nM). For the binding selectivity between quadruplex and duplex, **1** showed a 2.3-fold selectivity (3380 vs 1500 nM), **2** showed a 2.9-fold selectivity (482 vs 167 nM), while 3 showed an obviously higher selectivity of 8.4 fold (269 vs 32 nM).

Increase of Thermodynamic Stability of G-Quadruplex DNA by the Quindoline Derivatives. Thermodynamic stability of derivatives to G-quadruplex DNA was determined from the melting temperature of the G-quadruplex DNA using a FRET-melting assay.[30,42] In this assay, a truncated sequence of Pu39 named as MidG4 was used, which is consisted of four middle consecutive G-tracts of Pu39 sequence because the full-length Pu39 with complex conformation could affect the fluorophors. Actually, G-quadruplex formed by MidG4 has been proved to be the most stable and favorable G-quadruplex in Pu39 sequence.[12] The thermodynamic stability of MidG4 with the derivatives was measured from 37 to 99 °C in a LightCycler 2.0 apparatus (Roche), and the results of T_m values are listed in Table 3. Comparing with the control value without any derivatives (MidG4 T_m value of 48.5 °C), all the T_m values of samples incubated with the derivatives increased, indicating the quindoline derivatives could enhance the thermodynamic stability of this oligomer. **1** displayed the weakest stabilizing effect on *bcl-2* G-quadruplex, with only about 3 °C enhancement of T_m value. **2** could raise T_m value to 65 °C, while **3**, with the most potent stabilizing effect, could raise T_m value to 77 °C.

G-Quadruplex Formation Leads to Repression of *bcl-2*. First, we designed and synthesized two mutant of Pu39 sequences, MutPu39 and Mut1 (the sequence is listed in Figure 5), in order to eliminate the possibility for the formation of

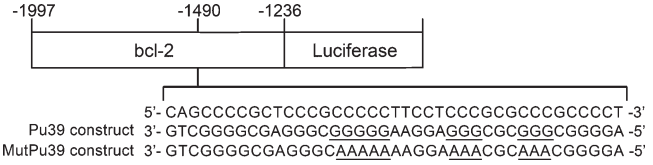

Figure 5. Constructs used in this paper for transient transfection experiments.

Table 4. Percentages of Luciferase Activity in Each Group Relative to Untreated Pu39 Construct Group

	Pu39 (%)	MutPu39 (%)	MutPu39 (%)[a]
no drug	100.0 ± 2.7	176.5 ± 7.2	100.0 ± 4.1
3	51.4 ± 5.8	131.7 ± 7.5	74.6 ± 4.3
2	70.5 ± 5.2	155.8 ± 5.0	88.3 ± 2.8
1	84.4 ± 4.1	163.4 ± 9.6	92.6 ± 5.4

[a] Percentage of luciferase activity relative to untreated MutPu39.

G-quadruplex in the *bcl-2* promoter region in vivo. For Mut1, G-to-A base mutations were made to one of central G-tract of Pu39, while three of G-tracts were mutated for MutPu39. Their conformations were further identified using CD spectroscopy (Supporting Information, Figure S3), which indicated that Pu39 oligomer could form a mixed parallel/antiparallel G-quadruplex. Mut1 oligomer still existed as parallel G-quadruplex structure, but MutPu39 oligomer showed complete disruption of G-quadruplex. On the basis of the above results, plasmids with wild-type Pu39 and MutPu39 mutation in promoter region were constructed as shown in Figure 5 to investigate the potential biological significance of the intramolecular G-quadruplex structures in *bcl-2* P1 promoter.

In the luciferase reporter assay, MutPu39 construct showed an approximately 2-fold increase of transcriptional activation than Pu39 construct in leukemia cell line HL-60 (Table 4). The above results indicate that the disruption of the G-quadruplex structure might cause an increase of transcriptional activation, and therefore this structure may act as a repressor element to transcriptional activation of *bcl-2*.

Turning Off Transcription of the *bcl-2* Gene in Vivo by Quindoline Derivatives. For the in vivo experiments, luciferase activity assay was carried out first in HL-60 cells. Two luciferase constructs were used in the assay, one was a Pu39 construct with the full-length wild promoter of *bcl-2* and the other was MutPu39 with the mutant promoter of Pu39 that could not form G-quadruplex. Figure 6 is a histogram displaying the effects of three derivatives on *bcl-2* promoter activity, and Table 4 gives the concrete percentages of luciferase activity after treatment with the derivatives. The addition of **3** (0.4 μM) resulted in about 50% reduction of luciferase activity for Pu39 construct, with 25% reduction for MutPu39 construct. The same concentration of **2** could also exert an inhibitory effect on luciferase activity of Pu39 and MutPu39 construct (30% vs 12%). However, the discriminations among the effects of 0.4 μM of **1** on different constructs were not statistically

significant. It inferred that the quindoline derivatives could inhibit the activity of *bcl-2* gene through their special interaction with the promoter region of Pu39. The activity of derivatives for binding and stabilizing G-quadruplex was in accordance with their ability for specifically inhibiting promoter activity of Pu39 construct. Moreover, the derivative **3** with the highest selectivity shown in SPR data showed a significant increase in its inhibition of promoter activity on Pu39 rather than MutPu39, while **1** could not show a significant difference for the two constructs.

Because of the weak inhibitory activity of **1** in luciferase activity assay, only **2** and **3** were chosen for the quantitative RT-PCR and Western blot assay. Total RNA from HL-60 cells was extracted and reversely transcribed to cDNA to investigate the effect of the derivatives on *bcl-2* gene transcription. The cDNA was then used as a template for specific real-time PCR amplification of *bcl-2* sequence with glyceraldehyde phosphate dehydrogenase (*GAPDH*) as a control. As shown in Figure 7, both derivatives, **2** and **3**, could dose-dependently decrease the related RNA of *bcl-2*. For translation of *bcl-2* gene, whole cell lysate of HL-60 cells was prepared and Bcl-2 protein was detected in Western blot analysis, with β-Actin as a control. As shown in Figure 8, both derivatives, **2** and **3**, could decrease the related protein products of *bcl-2* at increasing concentrations. The results suggested that the quindoline derivatives could down-regulate the transcription and translation of oncogene *bcl-2*. In addition, **3** was more effective than **2**, which was identified by using RT-PCR and Western blot. As for the results of real-time PCR shown in Figure 8, 0.2 μM of **3** led to a 50% decrease of *bcl-2* mRNA level, while 0.8 μM of **2** had a similar effect, also indicating **3** had a stronger activity of turning off *bcl-2* gene transcription. These observations were consistent with the results obtained in the PCR stop assay.

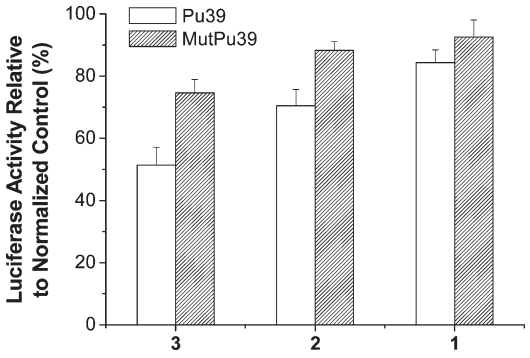

Figure 6. Effects of derivatives on *bcl-2* promoter activity. HL-60 cells were transient transfected with Pu39 plasmid or its mutant and pRL-TK and then treated with 0.4 μM of **3**, **2**, or **1** for 48 h. The efficiency of transfection was normalized by pRL-TK. Luciferase activity was plotted relative to the untreated group, which was assigned a value of 100%. Each data point was the average of three experiments. Error bars represent 1 SD above and below the mean relative activity.

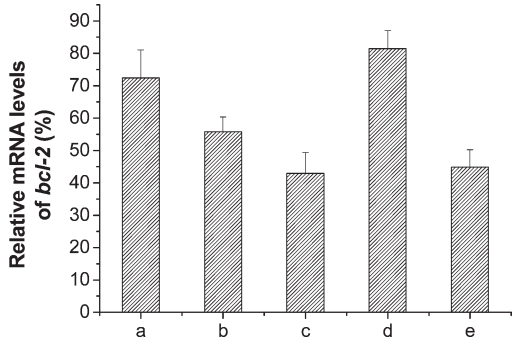

Figure 7. Relative expression level of *bcl-2* mRNA in drug-treated groups relative to untreated group, which was assigned a value of 100%. Bars a−c represented HL-60 cells treated with 0.2, 0.4, and 0.8 μM for **2**, while d and e represented cells treated with 0.1 and 0.2 μM for **3**, respectively. Each data point was the average of three experiments. Error bars represent 1 SD above and below the mean relative level.

Induction of HL-60 Cells Apoptosis by the Quindoline Derivatives. Proliferation assay was carried out with leukemia cell line HL-60 to evaluate the effect of quindoline derivatives on tumor cell apoptosis. According to the results from our pre-experiment (MTT assay, data not shown), the concentrations of 0.1, 0.2, 0.5, 1 μM for **2** and 0.02, 0.05, 0.1, 0.2 μM for **3** were used in the proliferation assay. As shown in Figure 9, both **2** and **3** could inhibit the proliferation of HL-60 cells, and the surviving cell number in the presence of **3** was less than that of **2** at the same concentration, indicating that **3** had a relatively strong inhibitory activity on proliferation.

HL-60 apoptosis induced by the two quindoline derivatives was determined with Western blot and flow cytometry assay[43] using similar drug concentrations as those in proliferation assay. Although the two derivatives showed certain cytotoxity on cells at a relative high concentration (1 μM for **2** and 0.2 μM for **3**), there was still at less 25% cells alive (as shown in Figure 9) and this was enough for the next assays. It has been well-known that caspase-3 mediates cleavage of many substrates, including poly ADP-ribose polymerase (PARP), and acted as a major executor of apoptosis.[44,45] Therefore, in the present study, we monitored caspase-3 and PARP proteins using Western blot method. Parts A and B of Figure 10 show that PARP was cleaved to an 89 kDa fragment after cells were treated with 1 μM of **2** or 0.2 μM of **3** for 4 days. As the derivatives concentration increased, cleavage of procaspase-3 (35 kDa) was observed, inferred by the weakening of the 35 kDa band. However, the caspase-3 fragmentations of 17 kDa were not detected, probably due to low protein concentration.

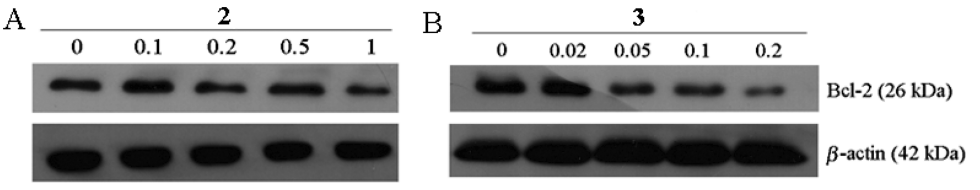

Figure 8. Effects of derivatives on *bcl-2* translation. (A) Western blot to determine the translation of *bcl-2* in HL-60 cell line treated with 0.1, 0.2, 0.5, 1 μM of **2** for 4 days. (B) Western blot to determine the translation of *bcl-2* in HL-60 cell line treated with 0.02, 0.05, 0.1, 0.2 μM of **3** for 4 days.

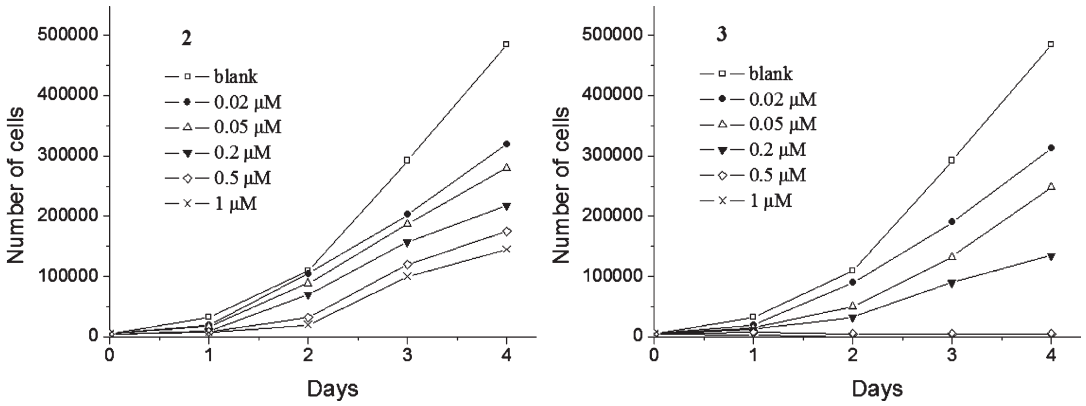

Figure 9. Effect of the quindoline derivatives (0.02, 0.05, 0.2, 0.5, and 1 μM) on HL-60 cell proliferation: 5×10^4 cells were seeded in microplate at day 0. Cell count and viability (trypan blue dye exclusion) were determined daily (from day 1 to day 4 of culture).

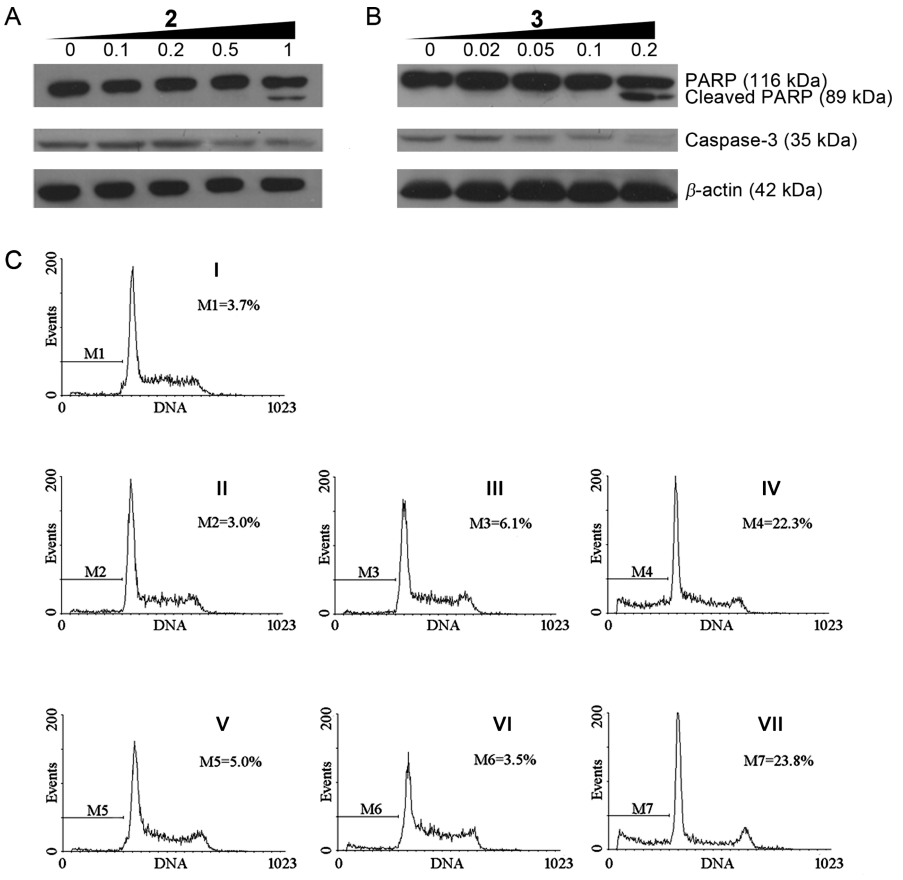

Figure 10. Apoptosis of HL-60 cells treated with quindoline derivatives. (A) Cleavage of caspase-3 and PARP of HL-60 cells treated with 0.1, 0.2, 0.5, 1 μM of **2** for 4 days. (B) Cleavage of caspase-3 and PARP of HL-60 cells treated with 0.02, 0.05, 0.1, 0.2 μM of **3** for 4 days. (C) HL-60 cells were treated with no drug (I), 0.2 μM (II), 0.5 μM (III), 1 μM (IV) of **2**, and 0.05 μM (V), 0.1 μM (VI), 0.2 μM (VII) of **3** for 4 days and then analyzed with flow cytometry. The M value represents the percent of apoptotic cells.

Using the flow cytometry assay, we found that the percentage of sub-G1 peak, representing the population of apoptosis cells, increased from 3% to 23% after treatment with 1 μM of **2** or 0.2 μM of **3** (Figure 10C, IV and VII). The results indicated that the two quindoline derivatives had significant activity to induce HL-60 cell apoptosis, and **3** was more effective than **2**.

Discussion

GC-rich regions, which could form G-quadruplex secondary structures, have been found to be widely existed in human gene promoters.[46,47] Among them, G-quadruplexes of several genes have been thoroughly investigated in vitro, however, little is known about their properties and functions in vivo. Even if G-quadruplex ligands could regulate the transcription of some genes, strong evidence for G-quadruplex as a transcriptional repressor has only been displayed in the promoter of *c-myc* gene using luciferase activity assay.[2] In the present study, we investigated the effect of G-quadruplex on the *bcl-2* transcription. The results showed an approximately 2-fold increase in transcriptional activity of the *bcl-2* promoter when G-quadruplex structure was totally disrupted by mutation

with G → A transition. These results verified the significant role of G-quadruplex in *bcl-2* P1 promoter on transcription in vivo.

Bcl-2 protein plays an important role as an apoptosis repressor, which is involved in the tumorigenesis and the progress of cancer.[48] Therefore, various selective *bcl-2* inhibitors have been discovered, such as antisense oligonucleotides to *bcl-2* gene[49] or peptidomimetics,[50] and small molecule inhibitors[51] to Bcl-2 protein. However, few studies about small molecules directly interacting to *bcl-2* gene have been published so far. Recently, some G-quadruplex ligands have been proved as apoptosis inducer.[52−54] In particular, the ligand 12459 had been found to induce apoptosis characterized by dysfunction of Bcl-2.[54] Besides, compound **4**, one of the quindoline derivatives, has been demonstrated to induce delayed-apoptosis in HL-60 cells.[32] In the present study, we chose three quindoline derivatives synthesized by our group which have different activity of stabilizing G-quadruplex and regulating related biological functions.[28−31] The aim of the present research was to demonstrate the interaction of the ligands with *bcl-2* gene and their induction of apoptosis. The difference in efficacy of the ligands was also compared in this study.

The interactions between the quindoline derivatives and the G-rich sequence in *bcl-2* gene (Pu39) were investigated using PCR stop assay, SPR and FRET-melting experiments. On the basis of these in vitro assays, the quindoline derivatives could bind to and stabilize the G-quadruplex structures formed in Pu39 sequence. Meanwhile, the activity of different quindoline derivatives to interact with G-rich DNA showed significant differences. **3**, a 7-fluorinated quindoline derivative methylated at the 5-N position and with an amino group side chain, showed the strongest binding/stabilizing activity, even in the presence of potassium. **2**, a quindoline derivative without 5-methylation comparing to **3**, had moderate activity. In comparison, the activity of **1**, a quindoline derivative with a hydroxyl group side chain, was the lowest by displaying little impact on G-quadruplex interaction. Moreover, when binding to G-quadruplex vs duplex structure, **3** had much better selectivity than other two derivatives.

On the basis of the results of luciferase activity in HL-60 cells, **3** and **2** were proved to have intensive activity of suppressing promoter in Pu39 construct rather than MutPu39. Similar to the structure−activity relationship of derivatives obtained from in vitro results, **3** had much more inhibitory effect on *bcl-2* promoter activity than **2**, while **1** could hardly exhibit statistically significant difference between *bcl-2* and mutated promoters. Upon the treatment of the quindoline derivatives **3** or **2** in HL-60 cells, transcription and translation of *bcl-2* gene was turned off; cell proliferation was inhibited and apoptosis was induced. Furthermore, **3** showed a relatively higher activity than **2**, consistent with the outcomes from in vitro and luciferase assays. To sum up, the induction/stabilization of G-quadruplex DNA by the quindoline derivatives influenced the biological events in which down-regulation of *bcl-2* gene was involved. Additionally, the comparative high selectivity of **3** binding to G-quadruplex resulted in a stronger effect on regulating *bcl-2* gene transcription and the following consequence.

The SAR results drawn from quindoline derivatives interaction with *bcl-2* G-quadruplex were in accordance with the previous results with telomeric or *c-myc* G-quadruplexes.[29−31] Therefore, this research gave a deeper examination of derivatives' functions on various G-quadruplex structures. It should be noted that apoptosis is a complicated intracellular suicide program, controlled by many internal and external factors. Therefore, our present experimental results may only show quindoline derivatives' apoptosis-inducing activity with relatively high cytotoxity, while other factors might also take part in controlling cell death induced by quindoline derivatives. Another result that should be paid attention to is that *bcl-2* promoter quadruplex was targeted by derivatives drawn from luciferase data, although the selectivity for quadruplex over duplex DNA was modest. Here, quindoline derivatives might exert their effects on *bcl-2* G-quadruplex with the assistance of various factors, such as metal ions, proteins, and so on, from much more complex in vivo environment (measuring promoter activity) than in vitro (determining selectivity).

In conclusion, this is the first time that the influence of G-quadruplex structures on the promoter activity of *bcl-2* gene has been demonstrated. Also, quindoline derivatives were verified with the activity of interacting/stabilizing *bcl-2* G-quadruplex structures, repressing promoter activity and inducing apoptosis in HL-60 cells. On the basis of the above results, in our future research, we plan to concentrate on developing novel derivatives with better binding selectivity (not only broadly for G-quadruplex vs duplex, but also specifically for *bcl-2* G-quadruplex vs other forms of G-quadruplex) and apoptosis-inducing activity. Inspecting the action of some typical small molecular ligands could present concrete evidence for molecular mechanism of apoptosis induction.

Materials and Methods

Chemicals. The quindoline derivatives, *N*′-(10*H*-indolo[3,2-*b*]-quinolin-11-ylamino)ethanol (**1**), *N*-(3-(dimethylamino)propyl)-7-fluoro-10*H*-indolo[3,2-*b*]quinolin-11-amine (**2**), and *N*′-(7-fluoro-5-*N*-methyl-10*H*-indolo[3,2-*b*]quinolin-5-ium)-*N*,*N*-dimethylpropane-1,3-diamine iodide (**3**), were synthesized by our group using a similar method as previously reported.[29,30] All of the compounds were identified by NMR, high-resolution mass spectra, and elemental analyses. Elemental analyses had been used to confirm ≥95% purity of compounds.

PCR Stop Assay. Sequences of the test oligomers (Pu39 or MutPu39) and the corresponding complementary sequence (Pu39rev) used are listed in Table 5. The reaction was performed in 1× PCR buffer, containing 2 μmol of each pair of oligomers, 0.16 mM dNTP, 2.5 U *Taq* polymerase, and derivatives at a certain concentration. Reaction mixtures were incubated in a thermocycler with the following cycling conditions: 94 °C for 3 min, followed by 10 cycles of 94 °C for 30 s, 58 °C for 30 s, and 72 °C for 30 s. Amplified products were resolved on 15% nondenaturing polyacrylamide gels in 1× TBE and ethidium bromide (EtBr) stained. IC_{50} values were calculated using optical density read from LabWorks software.

Surface Plasmon Resonance. SPR measurements were performed on a ProteOn XPR36 Protein Interaction Array system (Bio-Rad Laboratories, Hercules, CA) using a Neutravidin-coated NLC sensor chip. In a typical experiment, biotinylated duplex DNA and biotinylated Pu39 (Table 5) were folded in filtered and degassed running buffer (Tris-HCl 50 mM pH 7.4, 100 mM KCl). The DNA samples were then captured (∼1000 RU) in flow cells 1 and 2, leaving the third flow cell as a blank. Ligand solutions (at 7.81, 15.62, 31.25, 62.5, 125, 250, 500, 1000, and 2000 nM) were prepared with running buffer by serial dilutions from stock solutions. Six concentrations were injected simultaneously at a flow rate of 25 μL/min for 5 min of association phase, followed by 5 min of disassociation phase at 25 °C. The NLC sensor chip was regenerated with short injection of 1 M KCl between consecutive measurements. The final graphs were obtained by subtracting blank sensorgrams from the duplex or quadruplex sensorgrams. Data are analyzed with ProteOn manager software, using the Langmuir model for fitting kinetic data.

Table 5. Sequences of Oligomers/Primers Used in This Paper

name of oligomer	sequence
Pu39	5′-AGGGGCGGGCGCGGGAGGAAGGGGGCGGGAGCGGGGCTG-3′
Pu39rev	5′-ATCGATCGCTTCTCGTCAGCCCCGCT-3′
MutPu39	5′-AGGGGCAAACGCAAAAGGAAAAAAACGGGAGCGGGGCTG-3′
Mut1	5′-AGGGGCGGGCGCAAAAGGAAGGGGGCGGGAGCGGGGCTG-3′
biotinylated duplex DNA	5′-biotin-TTTTTTTTTCGAATTCGTTTTTCGAATTCG-3′
biotinylated Pu39	5′-biotin-AGGGGCGGGCGCGGGAGGAAGGGGGCGGGAGCGGGGCTG-3′
FMidG4T	5′-FAM-CGGGCGCGGGAGGAAGGGGGCGGGAGC-TAMRA-3′
Q*bcl-2* S	5′-GAGGATTGTGGCCTTCTTTG-3′
Q*bcl-2* A	5′-GCCGGTTCAGGTACTCAGTC-3′
Q*GAPDH* S	5′-GATGACATCAAGAAGGTGGTG-3′
Q*GAPDH* A	5′-GCTGTAGCCAAATTCGTTGTC-3′

FRET Assay. FRET assay was carried out on a real-time PCR apparatus (Roche LightCycler 2) following previously published procedures. The fluorescent labeled oligonucleotide FMidG4T (listed in Table 5), in which donor fluorophore FAM, 6-carboxyfluorescein, and acceptor fluorophore TAMRA, 6-carboxytetramethyl-rhodamine were used as the FRET probes, were diluted from stock to the correct concentration (200 nM) in Tris-HCl buffer (10 mM, pH 7.4) containing 100 mM KCl and then annealed by heating to 90 °C for 5 min, followed by cooling to room temperature. Samples were prepared by aliquoting 10 μL of the annealed FMidG4T (at 2× concentration, 400 nM) into LightCycler capillaries, followed by 10 μL of the compound solutions (at 2× concentration, 2 μM) and further incubated for 1 h. Measurements were made in triplicate on a real-time PCR with excitation at 470 nm and detection at 530 nm. Fluorescence readings were taken at intervals of 1 °C over the range 37−99 °C, with a constant temperature being maintained for 30 s prior to each reading to ensure a stable value. Final analysis of the data was carried out using Origin 7.5 (OriginLab Corp.).

Cell Culture and Treatment with Drugs. The HL-60 cell line was obtained from the American Type Culture Collection (ATCC) (Rockville, MD). The cell culture was maintained on RPMI-1640 medium supplemented with 10% fetal bovine serum, 100 U/mL penicillin and 100 μg/mL streptomycin in 25 cm^2 culture flasks at 37 °C humidified atmosphere with 5% CO_2. All cells to be tested in the following assays have a passage number of 3−6. For the drug treatment experiments, the HL-60 cells were harvested from the culture during exponential growth phase, seeded into multiwell culture plates at 5×10^4 cells/mL in fresh medium, and then treated with the derivatives at certain concentrations for 4 days.

Plasmid Construction. A DNA fragment from −1997 to −1236 of the human *bcl-2* gene promoter region, containing wild-type Pu39 sequence (from −1490 to −1451), was extracted from HL-60 cell total DNA by PCR. This fragment was then inserted into pMetLuc-Reporter Vector (Clontech), named Pu39 construct. As for MutPu39, site-directed mutations were made to the Pu39 region of the construct as shown in Figure 5.

Transfection and Luciferase Assays. DNA transfections were performed with HL-60 cells in log phase. First, 1.8 μg Pu39 or MutPu39 and 0.2 μg pRL-TK (Promega) were cotranfected into 2×10^6 HL-60 cells using Amaxa Cell Line Nucleofector Kit V (Lonza). Then, different concentrations of the derivative were added into medium after 4 h of transfection. After another 48 h drug treatment, the luciferase activity was evaluated by Ready-To-Glow Secreted Luciferase Reporter System (Clontech) and Renilla Luciferase Assay System (Promega).

RNA Extraction. Cell pellets harvested from each well of the culture plates were lysed in TRIzol solution. RNA was extracted with RNAiso Plus kit (Takara) according to manufacturer's protocol and eluted in distilled, deionized water with 0.1% diethyl pyrocarbonate (DEPC) to a final volume of 50 μL. RNA was quantitated spectrophotometrically and stored at −80 °C.

Real-Time PCR. Total RNA was used as a template for reverse transcription using the following protocol: each 20 μL reaction contained 1× M-MLV buffer, 125 μM dNTP, 100 pmol oligo dT_{18} primer, 100 units of M-MLV reverse transcriptase, DEPC in water (DEPC H_2O), and 2 μg of total RNA. Briefly, RNA and oligo dT_{18} primer was incubated at 70 °C for 10 min and then immediately placed on ice, after which the other components were added and incubated at 42 °C for 1 h and then at 70 °C for 15 min. Finally, the reacted solution was stored at −20 °C. Real-time PCR was performed on a real-time PCR apparatus (Roche LightCycler 2) by using SYBR Premix Ex *Taq* (Takara), according to the manufacturer's protocol. Primer sequences were shown in Table 5 (Q*bcl-2* S and Q*bcl-2* A for *bcl-2* gene, Q*GAPDH* S and Q*GAPDH* A for *GAPDH* gene). The total volume of 20 μL real-time RT-PCR reaction mixtures contained 10 μL of SYBR Premix Ex *Taq*, 0.4 μM each of forward and reverse primers, 1 μL of cDNA, and nuclease-free water. The program used for all genes consisted of a denaturing cycle of 3 min at 95 °C, 45 cycles of PCR (95 °C for 20 s, 58 °C for 30 s, and 68 °C for 30 s), a melting cycle consisting of 95 °C for 15 s, 65 °C for 15 s, and a step cycle starting at 65 °C with a 0.2 °C/s transition rate to 95 °C. The specificity of the real-time RT-PCR product was confirmed by melting curve analysis. The PCR product sizes were confirmed by agarose gel electrophoresis and ethidium bromide staining. Three replications were performed, and then *bcl-2* mRNA level was normalized to *GAPDH* mRNA level of each sample. Results of real-time PCR were analyzed using the $2^{-\Delta CT}$ method to compare the transcriptional levels of *bcl-2* genes in each sample relative to nondrug treated control.

Western Blot. Cells harvested from each well of the culture plates were lysed in 150 μL of extraction buffer consisting of 100 μL of solution A (50 mM glucose, 25 mM Tris-HCl, pH 8, 10 mM EDTA, 1 mM PMSF) and 50 μL of solution B (50 mM Tris-HCl, pH 6.8, 6 M urea, 6% 2-mercaptoethanol, 3% SDS, 0.003% bromphenol blue). The suspension was centrifuged at 10000 rpm at 4 °C for 5 min, and the supernatant (10 μL for each sample) was loaded onto 10% polyacrylamide gel and then transferred to a microporous polyvinylidene difluoride (PVDF) membrane. Western blotting was performed using anti-Bcl-2, anti-caspase-3, anti-PARP, or anti-β-actin antibody and horseradish peroxidase-conjugated antimouse or antirabbit secondary antibody. Protein bands were visualized using chemiluminescence substrate.

Flow Cytometry Analysis. Cells (10^6) were washed with ice-cold PBS and fixed in 75% ethanol at −20 °C for at least 1 h. After that, cells were washed twice, incubated with 0.5 mg/mL RNase A, and stained with 10 μg/mL propidium iodide (PI). Fluorescence emitted from the PI-DNA complex was quantitated by Epics Elite flow cytometry (Beckman-Coulter).

Acknowledgment. We thank the Natural Science Foundation of China (grants U0832005, 90813011, 20772159, 30801436), the Science Foundation of Guangzhou (2009A1-E011-6), the Ministry of Education of the People's Republic of China (grant 200805581163), and the Guangdong Natural Science Foundation (grant 8451008901000214) for financial support of this study.

Supporting Information Available: SPR sensorgrams for binding of quindoline derivatives to *bcl-2* G-quadruplex; FRET melting profiles of FMidG4T with quindoline derivatives; CD spectra for Pu39, Mut1 and MutPu39; fluorescence history of real-time PCR to detect mRNA level of *bcl-2* and *GAPDH* gene. This material is available free of charge via the Internet at http://pubs.acs.org.

References

(1) Hurley, L. H. Secondary DNA structures as molecular targets for cancer therapeutics. *Biochem. Soc. Trans.* **2001**, *29*, 692–696.
(2) Siddiqui-Jain, A.; Grand, C. L.; Bearss, D. J.; Hurley, L. H. Direct evidence for a G-quadruplex in a promoter region and its targeting with a small molecule to repress c-MYC transcription. *Proc. Natl. Acad. Sci. U.S.A.* **2002**, *99*, 11593–11598.
(3) Cogoi, S.; Xodo, L. E. G-quadruplex formation within the promoter of the KRAS proto-oncogene and its effect on transcription. *Nucleic Acids Res.* **2006**, *34*, 2536–2549.
(4) Qin, Y.; Rezler, E. M.; Gokhale, V.; Sun, D.; Hurley, L. H. Characterization of the G-quadruplexes in the duplex nuclease hypersensitive element of the PDGF-A promoter and modulation of PDGF-A promoter activity by TMPyP4. *Nucleic Acids Res.* **2007**, *35*, 7698–7713.
(5) Phan, A. T.; Kuryavyi, V.; Burge, S.; Neidle, S.; Patel, D. J. Structure of an unprecedented G-quadruplex scaffold in the human c-kit promoter. *J. Am. Chem. Soc.* **2007**, *129*, 4386–4392.
(6) Hsu, S. T.; Varnai, P.; Bugaut, A.; Reszka, A. P.; Neidle, S.; Balasubramanian, S. A G-rich sequence within the c-kit oncogene promoter forms a parallel G-quadruplex having asymmetric G-tetrad dynamics. *J. Am. Chem. Soc.* **2009**, *131*, 13399–409.
(7) Waller, Z. A.; Sewitz, S. A.; Hsu, S. T.; Balasubramanian, S. A small molecule that disrupts G-quadruplex DNA structure and enhances gene expression. *J. Am. Chem. Soc.* **2009**, *131*, 12628–33.
(8) Sun, D.; Liu, W. J.; Guo, K.; Rusche, J. J.; Ebbinghaus, S.; Gokhale, V.; Hurley, L. H. The proximal promoter region of the human vascular endothelial growth factor gene has a G-quadruplex structure that can be targeted by G-quadruplex-interactive agents. *Mol. Cancer Ther.* **2008**, *7*, 880–889.
(9) Guo, K.; Gokhale, V.; Hurley, L. H.; Sun, D. Intramolecularly folded G-quadruplex and i-motif structures in the proximal promoter of the vascular endothelial growth factor gene. *Nucleic Acids Res.* **2008**, *36*, 4598–608.
(10) Sun, D.; Guo, K.; Rusche, J. J.; Hurley, L. H. Facilitation of a structural transition in the polypurine/polypyrimidine tract within the proximal promoter region of the human VEGF gene by the presence of potassium and G-quadruplex-interactive agents. *Nucleic Acids Res.* **2005**, *33*, 6070–6080.
(11) Dexheimer, T. S.; Sun, D.; Hurley, L. H. Deconvoluting the Structural and Drug-Recognition Complexity of the G-Quadruplex-Forming Region Upstream of the bcl-2 P1 Promoter. *J. Am. Chem. Soc.* **2006**, *128*, 5404–5415.
(12) Dai, J.; Dexheimer, T. S.; Chen, D.; Carver, M.; Ambrus, A.; Jones, R. A.; Yang, D. An Intramolecular G-Quadruplex Structure with Mixed Parallel/Antiparallel G-Strands Formed in the Human BCL-2 Promoter Region in Solution. *J. Am. Chem. Soc.* **2006**, *128*, 1096–1098.
(13) De Armond, R.; Wood, S.; Sun, D.; Hurley, L. H.; Ebbinghaus, S. W. Evidence for the presence of a guanine quadruplex forming region within a polypurine tract of the hypoxia inducible factor 1alpha promoter. *Biochemistry* **2005**, *44*, 16341–16350.
(14) Guo, K.; Pourpak, A.; Beetz-Rogers, K.; Gokhale, V.; Sun, D.; Hurley, L. H. Formation of pseudosymmetrical G-quadruplex and i-motif structures in the proximal promoter region of the RET oncogene. *J. Am. Chem. Soc.* **2007**, *129*, 10220–10228.
(15) Palumbo, S. L.; Memmott, R. M.; Uribe, D. J.; Krotova-Khan, Y.; Hurley, L. H.; Ebbinghaus, S. W. A novel G-quadruplex-forming GGA repeat region in the c-myb promoter is a critical regulator of promoter activity. *Nucleic Acids Res.* **2008**, *36*, 1755–1769.
(16) Seto, M.; Jaeger, U.; Hockett, R. D.; Graninger, W.; Bennett, S.; Goldman, P.; Korsmeyer, S. J. Alternative promoters and exons, somatic mutation and deregulation of the Bcl-2-lg fusion gene in lymphoma. *EMBO J.* **1988**, *7*, 123–131.
(17) Heckman, C.; Mochon, E.; Arcinas, M.; Boxer, L. M. The WT1 protein is a negative regulator of the normal bcl-2 allele in t(14;18) lymphomas. *J. Biol. Chem.* **1997**, *272*, 19609–19614.
(18) Liu, Y. Z.; Boxer, L. M.; Latchman, D. S. Activation of the Bcl-2 promoter by nerve growth factor is mediated by the p42/p44 MAPK cascade. *Nucleic Acids Res.* **1999**, *27*, 2086–2090.
(19) Del Toro, M.; Bucek, P.; Avino, A.; Jaumot, J.; Gonzalez, C.; Eritja, R.; Gargallo, R. Targeting the G-quadruplex-forming region near the P1 promoter in the human BCL-2 gene with the cationic porphyrin TMPyP4 and with the complementary C-rich strand. *Biochimie* **2009**, *91*, 894–902.
(20) Li, H.; Liu, Y.; Lin, S.; Yuan, G. Spectroscopy probing of the formation, recognition, and conversion of a G-quadruplex in the promoter region of the bcl-2 oncogene. *Chemistry* **2009**, *15*, 2445–2452.
(21) Higashiyama, M.; Doi, O.; Kodama, K.; Yokouchi, H.; Tateishi, R. High prevalence of bcl-2 oncoprotein expression in small cell lung cancer. *Anticancer Res.* **1995**, *15*, 503–505.
(22) Harada, N.; Hata, H.; Yoshida, M.; Soniki, T.; Nagasaki, A.; Kuribayashi, N.; Kimura, T.; Matsuzaki, H.; Mitsuya, H. Expression of Bcl-2 family of proteins in fresh myeloma cells. *Leukemia* **1998**, *12*, 1817–1820.
(23) Leiter, U.; Schmid, R. M.; Kaskel, P.; Peter, R. U.; Krahn, G. Antiapoptotic bcl-2 and bcl-xL in advanced malignant melanoma. *Arch. Dermatol. Res.* **2000**, *292*, 225–232.
(24) Jacobson, M. D. Apoptosis: Bcl-2-related proteins get connected. *Curr. Biol.* **1997**, *7*, R277–281.
(25) Ohmori, T.; Podack, E. R.; Nishio, K.; Takahashi, M.; Miyahara, Y.; Takeda, Y.; Kubota, N.; Funayama, Y.; Ogasawara, H.; Ohira, T.; et al. Apoptosis of lung cancer cells caused by some anti-cancer agents (MMC, CPT-11, ADM) is inhibited by bcl-2. *Biochem. Biophys. Res. Commun.* **1993**, *192*, 30–36.
(26) Harima, Y.; Harima, K.; Shikata, N.; Oka, A.; Ohnishi, T.; Tanaka, Y. Bax and Bcl-2 expressions predict response to radiotherapy in human cervical cancer. *J. Cancer Res. Clin. Oncol.* **1998**, *124*, 503–510.
(27) Guittat, L.; Alberti, P.; Rosu, F.; Van Miert, S.; Thetiot, E.; Pieters, L.; Gabelica, V.; De Pauw, E.; Ottaviani, A.; Riou, J. F.; Mergny, J. L. Interactions of cryptolepine and neocryptolepine with unusual DNA structures. *Biochimie* **2003**, *85*, 535–547.
(28) Zhou, J. M.; Zhu, X. F.; Lu, Y. J.; Deng, R.; Huang, Z. S.; Mei, Y. P.; Wang, Y.; Huang, W. L.; Liu, Z. C.; Gu, L. Q.; Zeng, Y. X. Senescence and telomere shortening induced by novel potent G-quadruplex interactive agents, quindoline derivatives, in human cancer cell lines. *Oncogene* **2006**, *25*, 503–511.
(29) Zhou, J.-L.; Lu, Y.-J.; Ou, T.-M.; Zhou, J.-M.; Huang, Z.-S.; Zhu, X.-F.; Du, C.-J.; Bu, X.-Z.; Ma, L.; Gu, L.-Q.; Li, Y.-M.; Chan, A. S.-C. Synthesis and Evaluation of Quindoline Derivatives as G-Quadruplex Inducing and Stabilizing Ligands and Potential Inhibitors of Telomerase. *J. Med. Chem.* **2005**, *48*, 7315–7321.
(30) Lu, Y. J.; Ou, T. M.; Tan, J. H.; Hou, J. Q.; Shao, W. Y.; Peng, D.; Sun, N.; Wang, X. D.; Wu, W. B.; Bu, X. Z.; Huang, Z. S.; Ma, D. L.; Wong, K. Y.; Gu, L. Q. 5-*N*-Methylated quindoline derivatives as telomeric G-quadruplex stabilizing ligands: effects of 5-N positive charge on quadruplex binding affinity and cell proliferation. *J. Med. Chem.* **2008**, *51*, 6381–6392.
(31) Ou, T.-M.; Lu, Y.-J.; Zhang, C.; Huang, Z.-S.; Wang, X.-D.; Tan, J.-H.; Chen, Y.; Ma, D.-L.; Wong, K.-Y.; Tang, J. C.-O.; Chan, A. S.-C.; Gu, L.-Q. Stabilization of G-quadruplex DNA and down-regulation of oncogene *c-myc* by quindoline derivatives. *J. Med. Chem.* **2007**, *50*, 1465–1474.
(32) Liu, J.-N.; Deng, R.; Guo, J.-F.; Zhou, J.-M.; Feng, G.-K.; Huang, Z.-S.; Gu, L.-Q.; Zeng, Y.-X.; Zhu, X.-F. Inhibition of myc promoter and telomerase activity and induction of delayed apoptosis by SYUIQ-5, a novel G-quadruplex interactive agent in leukemia cells. *Leukemia* **2007**, *21*, 1300–1302.
(33) Guyen, B.; Schultes, C. M.; Hazel, P.; Mann, J.; Neidle, S. Synthesis and evaluation of analogues of 10*H*-indolo[3,2-*b*]-quinoline as G-quadruplex stabilising ligands and potential inhibitors of the enzyme telomerase. *Org. Biomol. Chem.* **2004**, *2*, 981–8.
(34) Caprio, V.; Guyen, B.; Opoku-Boahen, Y.; Mann, J.; Gowan, S. M.; Kelland, L. M.; Read, M. A.; Neidle, S. A novel inhibitor of human telomerase derived from 10*H*-indolo[3,2-*b*]quinoline. *Bioorg. Med. Chem. Lett.* **2000**, *10*, 2063–2066.
(35) Lemarteleur, T.; Gomez, D.; Paterski, R.; Mandine, E.; Mailliet, P.; Riou, J.-F. Stabilization of the c-myc gene promoter quadruplex by specific ligands' inhibitors of telomerase. *Biochem. Biophy. Res. Commun.* **2004**, *323*, 802–808.
(36) Teulade-Fichou, M.-P.; Carrasco, C.; Guittat, L.; Bailly, C.; Alberti, P.; Mergny, J.-L.; David, A.; Lehn, J.-M.; Wilson, W. D. Selective Recognition of G-Quadruplex Telomeric DNA by a Bis(quinacridine) Macrocycle. *J. Am. Chem. Soc.* **2003**, *125*, 4732–4740.
(37) Bugaut, A.; Jantos, K.; Wietor, J. L.; Rodriguez, R.; Sanders, J. K.; Balasubramanian, S. Exploring the differential recognition of DNA G-quadruplex targets by small molecules using dynamic combinatorial chemistry. *Angew. Chem., Int. Ed.* **2008**, *47*, 2677–2680.
(38) Read, M.; Harrison, R. J.; Romagnoli, B.; Tanious, F. A.; Gowan, S. H.; Reszka, A. P.; Wilson, W. D.; Kelland, L. R.; Neidle, S.

Structure-based design of selective and potent G quadruplex-mediated telomerase inhibitors. *Proc. Natl. Acad. Sci. U.S.A* **2001**, *98*, 4844–4849.
(39) Rezler, E. M.; Seenisamy, J.; Bashyam, S.; Kim, M.-Y.; White, E.; Wilson, W. D.; Hurley, L. H. Telomestatin and Diseleno Sapphyrin Bind Selectively to Two Different Forms of the Human Telomeric G-Quadruplex Structure. *J. Am. Chem. Soc.* **2005**, *127*, 9439–9447.
(40) Seenisamy, J.; Bashyam, S.; Gokhale, V.; Vankayalapati, H.; Sun, D.; Siddiqui-Jain, A.; Streiner, N.; Shinya, K.; White, E.; Wilson, W. D.; Hurley, L. H. Design and Synthesis of an Expanded Porphyrin That Has Selectivity for the c-MYC G-Quadruplex Structure. *J. Am. Chem. Soc.* **2005**, *127*, 2944–2959.
(41) Zhao, Y.; Kan, Z.-y.; Zeng, Z.-x.; Hao, Y.-h.; Chen, H.; Tan, Z. Determining the folding and unfolding rate constants of nucleic acids by biosensor. Application to telomere G-quadruplex. *J. Am. Chem. Soc.* **2004**, *126*, 13255–13264.
(42) Tan, J. H.; Ou, T. M.; Hou, J. Q.; Lu, Y. J.; Huang, S. L.; Luo, H. B.; Wu, J. Y.; Huang, Z. S.; Wong, K. Y.; Gu, L. Q. Isaindigotone derivatives: a new class of highly selective ligands for telomeric G-quadruplex DNA. *J. Med. Chem.* **2009**, *52*, 2825–2835.
(43) Crissman, H. A.; Steinkamp, J. A. Rapid, simultaneous measurement of DNA, protein, and cell volume in single cells from large mammalian cell populations. *J. Cell Biol.* **1973**, *59*, 766–771.
(44) Saraste, A.; Pulkki, K. Morphologic and biochemical hallmarks of apoptosis. *Cardiovasc. Res.* **2000**, *45*, 528–37.
(45) Soldani, C.; Scovassi, A. I. Poly(ADP-ribose) polymerase-1 cleavage during apoptosis: an update. *Apoptosis* **2002**, *7*, 321–328.
(46) Verma, A.; Yadav, V. K.; Basundra, R.; Kumar, A.; Chowdhury, S. Evidence of genome-wide G4 DNA-mediated gene expression in human cancer cells. *Nucleic Acids Res.* **2009**, *37*, 4194–4204.
(47) Verma, A.; Halder, K.; Halder, R.; Yadav, V. K.; Rawal, P.; Thakur, R. K.; Mohd, F.; Sharma, A.; Chowdhury, S. Genome-wide computational and expression analyses reveal G-quadruplex DNA motifs as conserved cis-regulatory elements in human and related species. *J. Med. Chem.* **2008**, *51*, 5641–5649.
(48) Lowe, S. W.; Lin, A. W. Apoptosis in cancer. *Carcinogenesis* **2000**, *21*, 485–495.
(49) Klasa, R. J.; Gillum, A. M.; Klem, R. E.; Frankel, S. R. Oblimersen Bcl-2 antisense: facilitating apoptosis in anticancer treatment. *Antisense Nucleic Acid Drug Dev.* **2002**, *12*, 193–213.
(50) Walensky, L. D.; Kung, A. L.; Escher, I.; Malia, T. J.; Barbuto, S.; Wright, R. D.; Wagner, G.; Verdine, G. L.; Korsmeyer, S. J. Activation of apoptosis in vivo by a hydrocarbon-stapled BH3 helix. *Science* **2004**, *305*, 1466–1470.
(51) Oltersdorf, T.; Elmore, S. W.; Shoemaker, A. R.; Armstrong, R. C.; Augeri, D. J.; Belli, B. A.; Bruncko, M.; Deckwerth, T. L.; Dinges, J.; Hajduk, P. J.; Joseph, M. K.; Kitada, S.; Korsmeyer, S. J.; Kunzer, A. R.; Letai, A.; Li, C.; Mitten, M. J.; Nettesheim, D. G.; Ng, S.; Nimmer, P. M.; O'Connor, J. M.; Oleksijew, A.; Petros, A. M.; Reed, J. C.; Shen, W.; Tahir, S. K.; Thompson, C. B.; Tomaselli, K. J.; Wang, B.; Wendt, M. D.; Zhang, H.; Fesik, S. W.; Rosenberg, S. H. An inhibitor of Bcl-2 family proteins induces regression of solid tumours. *Nature* **2005**, *435*, 677–681.
(52) Sumi, M.; Tauchi, T.; Sashida, G.; Nakajima, A.; Gotoh, A.; Shin-Ya, K.; Ohyashiki, J. H.; Ohyashiki, K. A G-quadruplex-interactive agent, telomestatin (SOT-095), induces telomere shortening with apoptosis and enhances chemosensitivity in acute myeloid leukemia. *Int. J. Oncol.* **2004**, *24*, 1481–1487.
(53) Leonetti, C.; Amodei, S.; D'Angelo, C.; Rizzo, A.; Benassi, B.; Antonelli, A.; Elli, R.; Stevens, M. F. G.; D'Incalci, M.; Zupi, G.; Biroccio, A. Biological activity of the G-quadruplex ligand RHPS4 (3,11-difluoro-6,8,13-trimethyl-8*H*-quino[4,3,2-*kl*]acridinium methosulfate) is associated with telomere capping alteration. *Mol. Pharmacol.* **2004**, *66*, 1138–1146.
(54) Douarre, C.; Gomez, D.; Morjani, H.; Zahm, J.-M.; O'Donohue, M.-F.; Eddabra, L.; Mailliet, P.; Riou, J.-F.; Trentesaux, C. Overexpression of Bcl-2 is associated with apoptotic resistance to the G-quadruplex ligand 12459 but is not sufficient to confer resistance to long-term senescence. *Nucleic Acids Res.* **2005**, *33*, 2192–2203.